

LETTER TO THE EDITOR

Structural and Electronic Factors Governing the Metallic and Nonmetallic Properties of the Pyrochlores $A_2Ru_2O_{7-y}$

K.-S. Lee

Department of Chemistry, The Catholic University of Korea, Puchon, Kyonggi-Do, South Korea 422-743

and

D.-K. Seo and M.-H. Whangbo¹

Department of Chemistry, North Carolina State University, Raleigh, North Carolina 27695-8204

Communicated by J. M. Honig March 10, 1997; accepted May 28, 1997

The metal-versus-semiconductor behavior of ruthenium pyrochlores $A_2Ru_2O_{7-y}$ was examined by calculating their electronic band structures. This behavior is explained in terms of the Mott–Hubbard mechanism of electron localization. The width of the t_{2g} -block bands of $A_2Ru_2O_{7-y}$ increases with increasing Ru–O–Ru bond angle, and the Ru–O–Ru angle increases with increasing size of the A cation. There is a good linear relationship between the ionic radius of the A cation and the Ru–O–Ru bond angle. This relationship makes it possible to calculate the amount of the O' atom vacancy based on the observed Ru–O–Ru angle in $Tl_2Ru_2O_{7-y}$. © 1997 Academic Press

INTRODUCTION

Ruthenium pyrochlores $A_2Ru_2O_{7-y}$ ($A = Bi, Pb, Tl$, rare earth, etc.) have been widely studied due to their technological importance (e.g., electrode materials (1), catalysts (2, 3), and components in thick film resistors (4)). They are metals or magnetic semiconductors depending on the A cations. There have been a number of attempts to find the structural origin of this metal-versus-semiconductor dichotomy (5–11). These studies indicate that the Ru–O–Ru bond angle is larger than 133° and $y > 0$ for metallic ruthenium pyrochlores $A_2Ru_2O_{7-y}$ (11). An electronic band structure study was carried out for metallic pyrochlores $Bi_2Ru_2O_7$ and $Pb_2Ru_2O_{6.5}$ (12), which revealed that the $6s$ and $6p$ bands of the A cations ($A = Bi, Pb$) lie below and above the Fermi level, respectively, and the metallic character originates from the Ru t_{2g} -block bands. In the present work, we probe

what structural and electronic factors make ruthenium pyrochlores metallic or semiconducting from the viewpoint of their electronic band structures, which we calculate using the extended Hückel tight binding method (13).

COORDINATE ENVIRONMENTS

The pyrochlore with the general formula $A_2B_2O_6O'$ has a structure in which distorted BO_6 octahedra share corners to form a tetrahedral lattice of the formula B_2O_6 (14). The A cations are present at the center of the hexagonal rings of oxygens (formed from six BO_6 octahedra) with two more oxygens (O') located above and below the ring and hence are eight-coordinate. Each O' atom is tetrahedrally coordinated with A cations, and the A and O' atoms form a tetrahedral lattice of the formula A_2O' . The B_2O_6 and A_2O' lattices interpenetrate, and the B and A cations interact through $B-O-A$ linkages. As indicated in Fig. 1, each O is surrounded with two B and two A cations in a distorted tetrahedron (local C_{2v} symmetry). The pyrochlore $A_2B_2O_6O'$ tolerates a high degree of vacancy on the O' anion sites, so its composition is $A_2B_2O_6(O')_{1-y}$, i.e., $A_2B_2O_{7-y}$ if the distinction between O and O' is not made.

ELECTRONIC BAND STRUCTURES

The ruthenium pyrochlores studied in our work include $Bi_2Ru_2O_7$ (7), $BiCaRu_2O_7$ (15), $PbNdRu_2O_7$ (10), $Tl_2Ru_2O_7$ (high and low temperature phases) (9), and $(RE)_2Ru_2O_7$ ($RE = Pr, Nd, Tb, Y, Yb$) (11, 16). The primary purpose of our EHTB calculations for ruthenium pyrochlores is to find the widths of their partially filled bands,

¹To whom correspondence should be addressed.

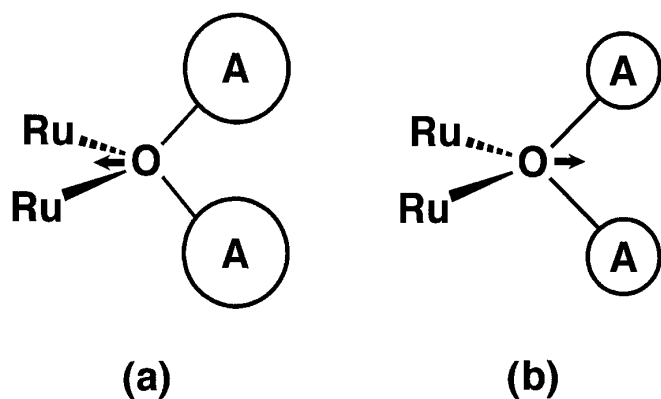


FIG. 1. Coordinate environment of the O atom in ruthenium pyrochlore $A_2Ru_2O_6O'$ showing the effect of the A cation size on the local structure: (a) a large A cation increases the Ru–O–Ru bond angle and shortens the Ru–O bond, and (b) a small cation decreases the Ru–O–Ru bond angle and lengthens the Ru–O bond.

i.e., the t_{2g} -block bands. If the Mott–Hubbard mechanism (17) of electron localization is applicable to these pyrochlores, then the bandwidths for metallic pyrochlores are expected to be wider than those for semiconducting ones. For our EHTB calculations, only the Ru_2O_6 sublattice was considered (i.e., the A_2O' sublattice was neglected) because our previous calculations for $Tl_2Mn_2O_7$ (18) revealed that the t_{2g} -block bands of the B_2O_6 sublattice are not strongly affected by the A_2O' sublattice. Figure 2 shows dispersion

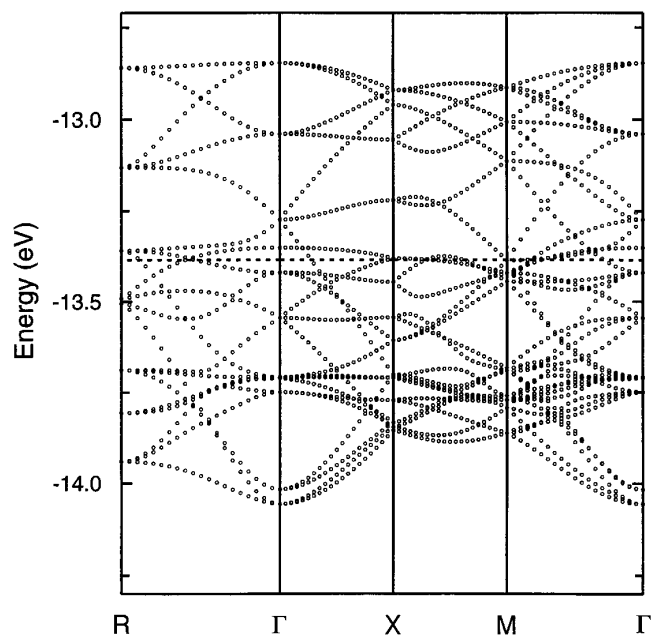


FIG. 2. Dispersion relations of the t_{2g} -block bands calculated for $Bi_2Ru_2O_7$. $\Gamma = (0, 0, 0)$, $X = (a^*/2, 0, 0)$, $M = (a^*/2, b^*/2, 0)$, and $R = (a^*/2, b^*/2, c^*/2)$.

relations of the t_{2g} -block bands calculated for $Bi_2Ru_2O_7$, where the overall width of the t_{2g} -block bands is determined by the lowest and highest points of the t_{2g} -block bands calculated at the Γ point. This is also the case for other ruthenium pyrochlores.

STRUCTURE–PROPERTY CORRELATIONS

Figure 3a plots the widths of the t_{2g} -block bands calculated for the ruthenium pyrochlores against their

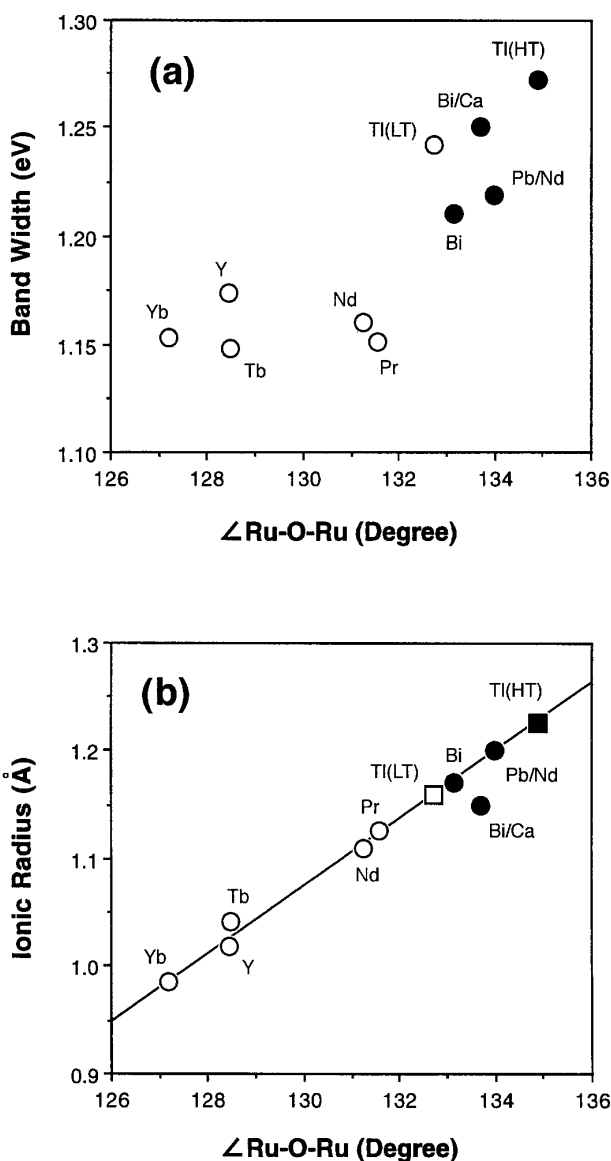


FIG. 3. (a) Widths of the t_{2g} -block bands versus the Ru–O–Ru bond angles in $A_2Ru_2O_{7-y}$. (b) Ionic radii of the A cations versus the Ru–O–Ru bond angles in $A_2Ru_2O_{7-y}$. Metallic and semiconducting phases are indicated by filled and empty circles, respectively. In (b), HT- and LT- $Tl_2Ru_2O_{7-y}$ are represented by filled and empty squares, respectively.

Ru–O–Ru bond angles, where the metallic and semiconducting compounds were indicated by filled and empty circles, respectively. Except for the case of the low-temperature phase of $\text{Tl}_2\text{Ru}_2\text{O}_7$ (9), the metallic and semiconducting phases are clearly separated in Fig. 3a. The metallic phases possess a wider bandwidth than do the semiconducting phases, so that the metal-versus-semiconductor dichotomy of the ruthenium pyrochlores is consistent with the Mott–Hubbard mechanism of electron localization. In general, for a solid made up of corner-sharing BO_6 octahedra, the t_{2g} orbitals of neighboring B atoms can have π -type orbital interactions through the B –O– B bridges (19). These interactions are enhanced by an increase in the B –O– B angle and a shortening of the B –O bond thereby increasing the overall width of the t_{2g} -block bands.

According to the environment of each O atom shown in Fig. 1a, it is expected that the larger the A cations, the farther the oxygen atoms will be pushed away from the A cations (along the bisector of the Ru–O–Ru angle), thereby increasing the Ru–O–Ru angle and shortening the Ru–O bond length. This reasoning predicts that a linear relationship is expected between the ionic radii of the A cations and the Ru–O–Ru bond angles. This is indeed the case, as shown in Fig. 3b, where eight-coordinate ionic radii (20) of the A cations (i.e., Bi^{3+} , Pb^{2+} , Ca^{2+} , RE^{3+}) were used, and the average of the two A cation radii was used for $\text{BiCaRu}_2\text{O}_{7-y}$ and $\text{PbNdRu}_2\text{O}_{7-y}$.

Since the Ru–O–Ru angles of high-temperature (HT) and low-temperature (LT) forms of $\text{Tl}_2\text{Ru}_2\text{O}_{7-y}$ are known, one can estimate their average Tl cation radii from the linear relationship of Fig. 3b (i.e., 1.230 and 1.156 Å for HT- and LT- $\text{Tl}_2\text{Ru}_2\text{O}_{7-y}$, respectively). In the $\text{Tl}_2\text{O}'$ sublattice, we assign the oxidation state of +3 to a Tl cation coordinated to two O' atoms, and +1 to a Tl cation coordinated to one O' atom. The reason for this assignment is that each of the four Tl^+ cations surrounding an O' vacancy has room to accommodate a lone pair (Fig. 4). Thus, for $\text{Tl}_2\text{Ru}_2\text{O}_{7-y}$ the ratio of the Tl^{3+} and Tl^+ cations is given by $(2 - 4y):4y$ assuming that each Tl is coordinated to at least one O' atom. The average Tl cation radii estimated from Fig. 3b are related to the weighted averages of the Tl^{3+} and Tl^+ cation radii (0.98 and 1.59 Å, respectively) with the relative weights

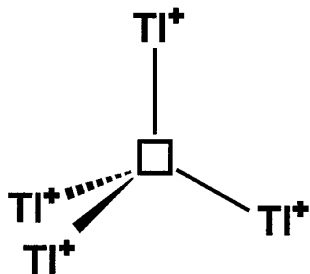


FIG. 4. Arrangement of four Tl^+ cations around a vacant O' site.

$(1 - 2y)$ and $2y$, respectively. Thus, the y value for HT- $\text{Tl}_2\text{Ru}_2\text{O}_{7-y}$ is calculated to be 0.21, which is in good agreement with the experimental value of 0.29 (9).

In a similar manner, the y value for LT- $\text{Tl}_2\text{Ru}_2\text{O}_{7-y}$ is calculated to be 0.15 from the linear relationship of Fig. 3b. This is in apparent contradiction to the reported experimental value ($y = 0.0$) (9). However, it is consistent with the observation from the X-ray photoelectron spectra of $\text{Tl}_2\text{Ru}_2\text{O}_{7-y}$ that the cell parameter of LT- $\text{Tl}_2\text{Ru}_2\text{O}_{7-y}$ (10.212 Å) lies in the region of metallic $\text{Tl}_2\text{Ru}_2\text{O}_{7-y}$ (> 10.188 Å) (5). It is probable that the powder samples of LT- $\text{Tl}_2\text{Ru}_2\text{O}_{7-y}$ used for neutron diffraction did have vacancy at the O' sites as predicted in our study. According to the correlation of Fig. 3a, the LT- $\text{Tl}_2\text{Ru}_2\text{O}_{7-y}$ phase is predicted to be metallic in disagreement with experiment. To account for this discrepancy, we present the following rationalization. The sintered pellet of LT- $\text{Tl}_2\text{Ru}_2\text{O}_{7-y}$ used for electrical resistivity measurements did indeed have no O' vacancy ($y = 0.0$) at least on the skins of the pellet. Then all of the Tl cations of the skin part of the lattice are in the +3 oxidation state, so that their ionic radius is small. This decreases the Ru–O–Ru bond angle and increases the Ru–O bond length (Fig. 1b), thereby reducing the width of the t_{2g} -block bands below the critical value.

CONCLUDING REMARKS

Our study shows that the metal-versus-semiconductor behavior of the ruthenium pyrochlores $\text{A}_2\text{Ru}_2\text{O}_{7-y}$ can be explained in terms of the Mott–Hubbard mechanism of electron localization. The width of the t_{2g} -block bands of $\text{A}_2\text{Ru}_2\text{O}_{7-y}$ increases with increasing Ru–O–Ru bond angle so that beyond a certain Ru–O–Ru angle the bandwidth becomes greater than a critical value, thereby making $\text{A}_2\text{Ru}_2\text{O}_{7-y}$ metallic. The Ru–O–Ru angle increases with increasing size of the A cation. There is a good linear relationship between the ionic radius of the A cation and the Ru–O–Ru bond angle. Using this relationship, it was possible to calculate the number of O' atom vacancies in LT- and HT- $\text{Tl}_2\text{Ru}_2\text{O}_{7-y}$.

ACKNOWLEDGMENTS

This work was supported by the U.S. Department of Energy, Office of Basic Sciences, Division of Materials Sciences, under Grant DE-FG05-86ER45259. Work at the Catholic University of Korea was supported by Grant C044677-I and by Grant BSRI-96-3421 from the Ministry of Education.

REFERENCES

1. R. G. Edgell, J. B. Goodenough, A. Hamnett, and C. C. Naish, *J. Chem. Soc. Faraday Trans. I* **79**, 893 (1983).
2. H. S. Horowitz, J. M. Longo, H. H. Horowitz, and J. T. Lewandowski, *ACS Symp. Ser.* **127**, 143 (1985).

3. T. R. Felthouse, P. B. Fraundorf, R. M. Friedman, and C. L. Schosser, *J. Catal.* **127**, 421 (1991).
4. P. F. Garcia, A. Ferreti, and A. Suna, *J. Appl. Phys.* **53**, 5282 (1982).
5. H. S. Jarrett, A. W. Sleight, J. F. Weiher, J. L. Gillson, C. G. Frederick, G. A. Jones, R. S. Swingle, D. Swatzfager, J. E. Gulley, and P. C. Hoell, in "Valence Instabilities and Related Narrow Band Phenomena" (R. D. Parks, Ed.), p. 545. Plenum, New York, 1977.
6. P. A. Cox, J. B. Goodenough, P. J. Tavener, D. Telles, and R. G. Edgell, *J. Solid State Chem.* **62**, 360 (1986).
7. G. Facer, M. M. Elcombe, and B. J. Kennedy, *Aust. J. Chem.* **46**, 1897 (1993).
8. R. Kanno, Y. Takeda, T. Yamamoto, Y. Kawamoto, and O. Yamamoto, *J. Solid State Chem.* **102**, 106 (1993).
9. R. Kanno, J. Huang, and A. W. Sleight, in "Proceedings of the Fifth International Symposium on Advanced Nuclear Energy Research," p. 127. 1994.
10. H. Kobayashi, R. Kanno, Y. Kawamoto, T. Kamiyama, F. Izumi, and A. W. Sleight, *J. Solid State Chem.* **114**, 15 (1995).
11. B. J. Kennedy and T. Vogt, *J. Solid State Chem.* **126**, 261 (1996). [See references therein]
12. W. Y. Hsu, R. V. Kasowski, T. Miller, and T. C. Chang, *Appl. Phys. Lett.* **52**, 792 (1988).
13. M.-H. Whangbo and R. Hoffmann, *J. Am. Chem. Soc.* **100**, 6093 (1978).
14. M. A. Subramanian, G. Aravamudan, and G. V. Subba Rao, *Prog. Solid State Chem.* **15**, 55 (1983). [See references cited therein]
15. B. J. Kennedy, *J. Solid State Chem.* **119**, 254 (1995).
16. B. J. Kennedy, *Acta Crystallogr. Sect. C* **51**, 790 (1995).
17. N. F. Mott, "Metal-Insulator Transitions." Barnes and Noble, New York, 1977.
18. D.-K. Seo, M.-H. Whangbo, and M. A. Subramanian, *Solid State Commun.* **101**, 417 (1997).
19. E. Canadell and M.-H. Whangbo, *Chem. Rev.* **91**, 965 (1991).
20. R. D. Shannon, *Acta Crystallogr. A* **32**, 751 (1976).